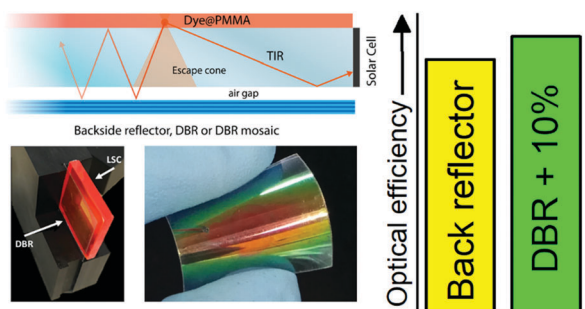


We have presented the Graphical Abstract text and image for your article below. This brief summary of your work will appear in the contents pages of the issue in which your article appears.



### Luminescent solar concentrators: boosted optical efficiency by polymer dielectric mirrors

G. Iasilli, R. Francischello, P. Lova, S. Silvano, A. Surace, G. Pesce, M. Alloisio, M. Patrini, M. Shimizu, D. Comoretto\* and A. Pucci\*

High dielectric contrast polymer distributed Bragg reflectors are used to recycle non-absorbed photons in organic luminescent solar concentrators. A 10% increase in the concentrator optical efficiency is found and retained upon doubling its size. These results pave the way to building lightweight and cheap integrated photovoltaic systems.

Please check this proof carefully. Our staff will not read it in detail after you have returned it.

Please send your corrections either as a copy of the proof PDF with electronic notes attached or as a list of corrections. **Do not edit the text within the PDF or send a revised manuscript** as we will not be able to apply your corrections. Corrections at this stage should be minor and not involve extensive changes.

**Proof corrections must be returned as a single set of corrections, approved by all co-authors. No further corrections can be made after you have submitted your proof corrections as we will publish your article online as soon as possible after they are received.**

Please ensure that:

- The spelling and format of all author names and affiliations are checked carefully. You can check how we have identified the authors' first and last names in the researcher information table on the next page. **Names will be indexed and cited as shown on the proof, so these must be correct.**
- Any funding bodies have been acknowledged appropriately and included both in the paper and in the funder information table on the next page.
- All of the editor's queries are answered.
- Any necessary attachments, such as updated images or ESI files, are provided.

Translation errors can occur during conversion to typesetting systems so you need to read the whole proof. In particular please check tables, equations, numerical data, figures and graphics, and references carefully.

Please return your **final** corrections, where possible within **48 hours** of receipt, by e-mail to: MaterChemFrontiersPROD@rs-c.org. If you require more time, please notify us by email.

## Funding information

Providing accurate funding information will enable us to help you comply with your funders' reporting mandates. Clear acknowledgement of funder support is an important consideration in funding evaluation and can increase your chances of securing funding in the future.

We work closely with Crossref to make your research discoverable through the Funding Data search tool (<http://search.crossref.org/funding>). Funding Data provides a reliable way to track the impact of the work that funders support. Accurate funder information will also help us (i) identify articles that are mandated to be deposited in **PubMed Central (PMC)** and deposit these on your behalf, and (ii) identify articles funded as part of the **CHORUS** initiative and display the Accepted Manuscript on our web site after an embargo period of 12 months.

Further information can be found on our webpage (<http://rsc.li/funding-info>).

### What we do with funding information

We have combined the information you gave us on submission with the information in your acknowledgements. This will help ensure the funding information is as complete as possible and matches funders listed in the Crossref Funder Registry.

If a funding organisation you included in your acknowledgements or on submission of your article is not currently listed in the registry it will not appear in the table on this page. We can only deposit data if funders are already listed in the Crossref Funder Registry, but we will pass all funding information on to Crossref so that additional funders can be included in future.

### Please check your funding information

The table below contains the information we will share with Crossref so that your article can be found *via* the Funding Data search tool. **Please check that the funder names and grant numbers in the table are correct and indicate if any changes are necessary to the Acknowledgements text.**

Funder name	Funder's main country of origin	Funder ID (for RSC use only)	Award/grant number
Università di Pisa	Italy	501100007514	BIHO 2017, PRA 2017 (project No. 2017_28)
Università degli Studi di Genova	Italy	501100004702	Unassigned
H2020 Marie Skłodowska-Curie Actions	European Union	100010665	643238

## Researcher information

Please check that the researcher information in the table below is correct, including the spelling and formatting of all author names, and that the authors' first, middle and last names have been correctly identified. **Names will be indexed and cited as shown on the proof, so these must be correct.**

If any authors have ORCID or ResearcherID details that are not listed below, please provide these with your proof corrections. Please ensure that the ORCID and ResearcherID details listed below have been assigned to the correct author. Authors should have their own unique ORCID iD and should not use another researcher's, as errors will delay publication.

Please also update your account on our online [manuscript submission system](#) to add your ORCID details, which will then be automatically included in all future submissions. See [here](#) for step-by-step instructions and more information on author identifiers.

First (given) and middle name(s)	Last (family) name(s)	ResearcherID	ORCID iD
G.	Iasilli		
R.	Francischello		
P.	Lova	V-8842-2018	0000-0002-5634-6321
S.	Silvano		
A.	Surace		
G.	Pesce		
M.	Alloisio		
M.	Patrini		
M.	Shimizu		0000-0002-3267-4902

D.	Comoretto	F-3418-2012	0000-0002-2168-2851
A.	Pucci	E-7453-2010	0000-0003-1278-5004

## Queries for the attention of the authors

Journal: **Materials Chemistry Frontiers**

Paper: **c8qm00595h**

Title: **Luminescent solar concentrators: boosted optical efficiency by polymer dielectric mirrors**

For your information: You can cite this article before you receive notification of the page numbers by using the following format: (authors), Mater. Chem. Front., (year), DOI: 10.1039/c8qm00595h.

Editor's queries are marked on your proof like this **Q1**, **Q2**, etc. and for your convenience line numbers are indicated like this 5, 10, 15, ...

Please ensure that all queries are answered when returning your proof corrections so that publication of your article is not delayed.

Query reference	Query	Remarks
Q1	Please confirm that the spelling and format of all author names is correct. Names will be indexed and cited as shown on the proof, so these must be correct. No late corrections can be made.	
Q2	Please check that the Graphical Abstract text fits within the allocated space indicated on the front page of the proof. If the entry does not fit between the two horizontal lines, then please trim the text and/or the title.	
Q3	The sentence beginning "On the other hand. . ." has been altered for clarity. Please check that the meaning is correct.	
Q4	Ref. 3: Please provide the full list of author names (including initials) and/or full list of editor names (including initials).	
Q5	Please provide full details for ref. 10 and 47.	
Q6	Ref. 25: Please provide the title/journal title if a journal article, page or article number(s).	
Q7	Ref. 36: Can this reference be updated? If so, please provide the relevant information such as year, volume and page or article numbers as appropriate.	

## RESEARCH ARTICLE

# Luminescent solar concentrators: boosted optical efficiency by polymer dielectric mirrors†

Cite this: DOI: 10.1039/c8qm00595h

 G. Iasilli,<sup>a</sup> R. Francischello,<sup>a</sup> P. Lova,<sup>b</sup> S. Silvano,<sup>b</sup> A. Surace,<sup>b</sup> G. Pesce,<sup>b</sup> M. Alloisio,<sup>b</sup> M. Patrini,<sup>c</sup> M. Shimizu,<sup>d</sup> D. Comoretto<sup>ib</sup>\*<sup>b</sup> and A. Pucci<sup>id</sup>\*<sup>a</sup>

We report on the optical efficiency enhancement of luminescent solar concentrators based on a push-pull fluorophore realized using high dielectric contrast polymer distributed Bragg reflectors as back mirrors. The Bragg stacks are obtained by alternating layers of cellulose acetate and thin films of a new stable and solution processable hydrated titania–poly(vinyl alcohol) nanocomposite (HyTiPVA) with a refractive index greater than 1.9 over a broad spectral range. The results obtained with these systems are compared with enhancements provided by standard Bragg reflectors made of commercial polymers. We demonstrate that the application of the Bragg stacks with photonic band-gap tuned to the low energy side of the dye emission spectrum induces a 10% enhancement of optical efficiency. This enhancement is the result of a photon recycling mechanism and is retained even in a scaled-up device where the Bragg mirrors are used in a mosaic configuration.

 Received 20th November 2018,  
 Accepted 18th December 2018

DOI: 10.1039/c8qm00595h

rsc.li/frontiers-materials

## Introduction

Nowadays, cost reduction and efficiency enhancement are the driving forces for technological development of photovoltaic (PV) systems.<sup>1</sup> In recent years, luminescent solar concentrators (LSCs) have become appealing thanks to their light weight, high concentration factors, and the possibility of operating with diffuse light without the need for expensive solar trackers and coolers.<sup>2</sup> Moreover, these devices can be easily integrated into modern constructions and, together with other systems for energy saving, such as adaptive windows,<sup>3,4</sup> could allow zero energy consumption buildings, accordingly to the EU guideline 2010/31/UE for 2020.

Even though LSCs are already available on the market,<sup>5</sup> some drawbacks are still limiting their massive commercial distribution. Such drawbacks include difficulties in the preparation of easily mountable modules and in the improvement of the device efficiency, which can be understood by analyzing their working principle. LSCs are highly transparent, planar

and relatively thick waveguides doped with high quantum yield fluorophores.<sup>2</sup> The slabs have a refractive index higher than their surroundings. In this way they favor total internal reflection of light emitted within the slab and its guiding to its sides, where standard solar cells are placed.<sup>2</sup> Notwithstanding their simplicity, several processes rule and limit their global device efficiency ( $\eta_{\text{dev}}$ ), including the usually poor matching between the fluorophore absorption spectrum and the solar emission ( $\eta_{\text{ABS}}$ ) as well as the dye emission efficiency ( $\eta_{\text{PL}}$ ). Besides the issues related to the fluorophore, the efficiency of the lateral solar cells ( $\eta_{\text{PV}}$ ), the waveguiding process ( $\eta_{\text{WG}}$ ), and the trapping process ( $\eta_{\text{trap}}$ ) affect the entire energy generation process such that:

$$\eta_{\text{dev}} = \eta_{\text{ABS}}\eta_{\text{PL}}\eta_{\text{WG}}\eta_{\text{PV}}\eta_{\text{trap}} \quad (1)$$

Concerning  $\eta_{\text{ABS}}$ , several researchers have focused on the development of new fluorophores with high spectral absorption and on tuning such absorption in the near infrared part of the solar spectrum, while maintaining the device transparency.<sup>2,6–8</sup> To this end, high efficiency quantum dots synthesized without the commonly used toxic heavy metals are very promising.<sup>6</sup> Conversely, if colored LSCs are chosen for aesthetic purposes, the efficiency can be increased by using smart near infrared scatterers to funnel the non-absorbed long-wavelength solar radiation into the waveguide.<sup>9,10</sup> Regarding  $\eta_{\text{PL}}$ , several dyes with quantum yield close to unity have been proposed.<sup>2</sup> On the other hand, self-absorption effects hinder  $\eta_{\text{PL}}$ , especially when devices with large surface areas and high fluorophore concentrations are used. This drawback has been widely addressed by engineering the fluorophore to maximize the Stokes shift.

<sup>a</sup> Dipartimento di Chimica e Chimica Industriale, Università di Pisa, via Moruzzi 13, 56124 Pisa, Italy. E-mail: davide.comoretto@unige.it

<sup>b</sup> Dipartimento di Chimica e Chimica Industriale, Università di Genova, Via Dodecaneso 31, 16146 Genova, Italy. E-mail: andrea.pucci@unipi.it

<sup>c</sup> Dipartimento di Fisica, Università di Pavia, via Bassi 6, 27100 Pavia, Italy

<sup>d</sup> Faculty of Molecular Chemistry and Engineering, Kyoto Institute of Technology, 606-8585 Kyoto, Japan

† Electronic supplementary information (ESI) available: Hybrid titania–PVA nanocomposite optical constants (S1); diffuser and LSC characterization (S2); optical characterization of the DBRs (S3); and optical efficiency measurement details (S4). See DOI: 10.1039/c8qm00595h

Moreover, Förster energy transfer has been investigated for molecular fluorophores, but the need to achieve proper blending on large area makes their use challenging.<sup>2</sup> To this end, donor–acceptor core–shell quantum dots are promising thanks to the possibility of coupling different materials and achieving large Stokes shifts by simple wet chemistry.<sup>6,11,12</sup> The use of fluorogenic dye exploiting molecular aggregation or push–pull molecules could be an alternative approach to the problem.<sup>13–16</sup> Then, while molecular aspects, photoluminescence, and device efficiencies have been widely addressed and understood,<sup>2,17,18</sup> many strategies are still under investigation for the enhancement of  $\eta_{\text{trap}}$ .<sup>19</sup> In this work, we propose a new approach to enhance this parameter, while leaving the other efficiencies unchanged. For a waveguide with refractive index  $n_{\text{slab}} \sim 1.5$ ,  $\eta_{\text{trap}}$  is evaluated as:

$$\eta_{\text{trap}} = \sqrt{1 - \left(\frac{n_{\text{air}}}{n_{\text{slab}}}\right)^2} \simeq 0.74 \quad (2)$$

which means that almost 26% of photons emitted by the fluorophore leave the slab within the escape cone and do not reach the lateral sides of the waveguide where the solar cells are placed (Fig. 1(a)). So far, the lost photons have been recycled using different reflectors including diffusive back reflectors, complex mirroring systems using plasmonic structures,<sup>19–23</sup> rugate filters, or opal-like photonic crystals with photonic band gap (PBG) tuned on the emission spectrum.<sup>21,24–26</sup> More recently, front and back reflectors have been modelled<sup>27</sup> and applied to LSCs embedding micro-solar cells into the waveguide.<sup>28</sup>

In this work, we report on the role of polymer distributed Bragg reflectors (DBR) as back mirror – in place of a standard diffuser – on the performances of LSCs (Fig. 1(b and c)). Polymer DBRs and related structures with very high reflectance in a limited spectral region have been already exploited for

lasing, fluorescence emission control, optical switches, and sensors.<sup>29–37</sup> The optical responses of DBR, including the spectral position of the photonic band-gap, its reflectance intensity and bandwidth, are mainly dictated by the periodicity of the structure and the refractive index contrast among the polymer components.<sup>36</sup> Here, in order to increase the reflection bandwidth, we spun-cast high dielectric contrast polymer DBRs properly tuned to enhance the LSC performances. The DBRs allowed a  $\sim 10\%$  enhancement of the optical efficiency that is retained also on scaled-up devices through mosaicking of the DBRs. To this end, we employed both polymer DBRs fabricated alternating commercial cellulose acetate (CA) and poly(*N*-vinyl carbazole) (PVK) layers (sample series P), or CA and the novel processable hydrated titania–poly(vinyl alcohol) nanocomposites (HyTiPVA) with a very high refractive index (sample series H).

## Experimental section

### Fluorophore synthesis and characterization

SilaFluo was synthesized according to the literature.<sup>17,38</sup> Absorption and reflectance spectra were measured at room temperature by an Agilent Cary5000 UV-Vis-NIR spectrophotometer equipped with an Internal Diffuse Reflectance DRA-2500. Fluorescence spectra were measured at room temperature by a Horiba Jobin-Yvon Fluorolog<sup>®</sup>-3 spectrofluorometer equipped with a 450 W Xenon arc lamp and single and double grating excitation and emission monochromators, respectively.

### LSC preparation

To prepare the fluorophore–PMMA layer, about 30 mg of PMMA and SilaFluo were dissolved in  $\sim 0.8$  mL of chloroform and stirred for 30 min at room temperature. Subsequently, the solution was spread out evenly on a thoroughly cleaned  $35 \times 50$  mm glass surface to obtain a film with thickness  $25 \pm 5$   $\mu\text{m}$  (Starrett micrometer) after evaporation at room temperature in a closed environment. The polymer film was then removed after immersion in water and stored in a desiccator for successive measurements by attaching them on  $24 \times 24 \times 3$  mm (geometrical factor,  $G = 8$ ) or  $50 \times 50 \times 3$  mm ( $G = 16.7$ ) cleaned glass (Edmund Optics Ltd BOROFLOAT window) with a high-purity silicone oil (poly(methylphenyl siloxane), 710 fluid, Aldrich,  $n = 1.5365$ ) layer. The diffuser and the DBRs or DBR mosaic (4 DBRs) were placed beneath the LSC with  $G = 8$  ( $G = 16.7$ ).

### Preparation of HyTiPVA

The HyTiPVA composite was prepared by mixing aqueous solutions of PVA and HyTi with different concentrations adapting a wet synthetic protocol previously reported.<sup>39</sup> HyTi solutions were previously obtained through a controlled hydrolysis of commercial  $\text{TiCl}_4$  (Sigma-Aldrich, purity  $> 99\%$ ) by slow addition of 8 mL of  $\text{TiCl}_4$  cooled at  $0$  °C with ice to 62.5 mL of water. The mixtures were maintained under constant stirring at room temperature for 12 h to ensure full reaction. A clear colorless HyTi solution with a Ti concentration of 1.03 mmol

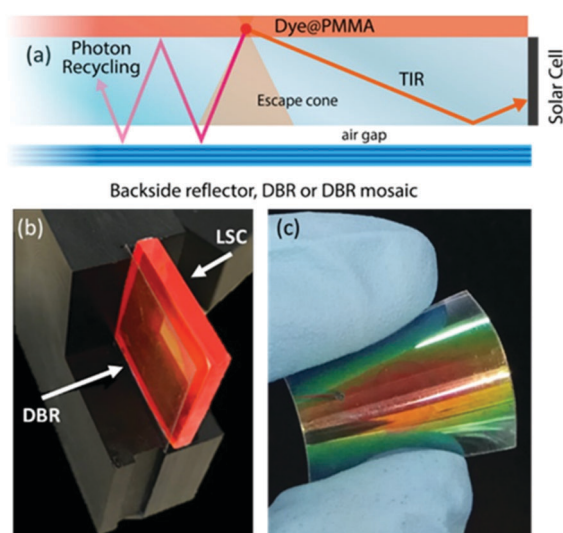


Fig. 1 (a) Schematic of the LSC configuration and main processes involved. Digital photograph of (b) the LSC device coupled to a DBR and (c) of a flexible DBR.

$L^{-1}$  was obtained. To produce the hybrid material, the freshly prepared HyTi solutions were added to a  $20 \text{ g L}^{-1}$  aqueous solution of PVA (Sigma-Aldrich, ( $M_n$ ) =  $1.66 \times 10^5 \text{ g mol}^{-1}$ , 99+% hydrolyzed) at a constant ratio of 1.4 : 1 v/v). The samples were transparent in the vis-NIR spectral interval (Fig. S1, ESI<sup>†</sup>) and solution processable for the preparation of spin-coated films. For this purpose, the filmability of hybrid solutions was optimized by the addition of EtOH in the ratio of 1 : 2 v/v before the mixture deposition.

### Polymer DBRs

P series DBRs were prepared by spin-coating CA (Aldrich,  $M_n = 30\,000$ ) dissolved in diacetone alcohol ( $35 \text{ mg mL}^{-1}$ ) and PVK (ACROS Organic,  $M_n = 56\,400$ ,  $M_w = 135\,600$ ) in toluene solutions ( $28 \text{ mg mL}^{-1}$ ) on poly(ethylene terephthalate) (PET) substrates; the rotation speed was kept between 80 and 105 RPS. H series DBRs were prepared by casting alternate layers of HyTi/PVA and the CA solution on glass substrates with rotation speed ranging between 80 and 120 RPS. More details are reported in Table S1 (ESI<sup>†</sup>).

### Optical efficiency of LSCs

The optical efficiency of the LSC was measured with a home-built equipment setup. Each DBR, single or mosaic, was placed beneath the LSC of  $G = 8$  or  $G = 16$ , respectively. Each sample was tested in triplicate. A solar simulating lamp (ORIEL<sup>®</sup> LCS-100 solar simulator 94011A S/N: 322, AM 1.5G std filter:  $69 \text{ mW cm}^{-2}$  at 254 mm) was housed 27.5 cm above the sample. The PV module (IXYS SLMD121H08L mono solar cell  $86 \times 14 \text{ mm}$ ) was connected to a digital potentiometer (AD5242) controlled *via* I2C by an Arduino Uno micro-controller using I2C master library.<sup>40</sup> A digital multimeter (KEITHLEY 2010) was connected in series with the circuit, between the photovoltaic module and the potentiometer, to collect the current as a function of the external load. Conversely, the voltage was measured by connecting the multimeter in parallel to the digital potentiometer.

### Optical function characterization

Spectroscopic ellipsometry measurements have been performed on reference thin films of the different materials, by using a VASE instrument by J. A. Woollam Co. in the range 250–2500 nm at different angles of incidence from  $60^\circ$  to  $75^\circ$ .<sup>41</sup> Transmittance at normal incidence has also been measured with a Varian Cary 6000i spectrometer in the spectral range 300–1800 nm. As a result, the complex refractive index  $n + ik$  for all materials was evaluated by WVASE32<sup>®</sup> software, adopting oscillator models that guarantee Kramers–Kronig consistency and effective-medium approximation for the HyTi/PVA nanocomposite.

## Results and discussion

The standard LSC devices were fabricated casting a thin layer of poly(methyl methacrylate) (PMMA) doped with a SilaFluo fluorophore on a glass slab. Then, a diffuser layer was applied to the

back of the slab with an air gap (Fig. 1, see Fig. S1 (ESI<sup>†</sup>) for the optical characterization of the diffuser and the slab). As mentioned before, the air gap guarantees that the slab guiding properties are maintained. This system represents the reference LSC. In our improved LSC devices, the diffuser was replaced with different Bragg stacks maintaining the air gap, as described in the Experimental section.

The fluorophore used in this work is a red-emitting 2-amino-7-acceptor-9-silafluorene, where the amino group  $-N(\text{CH}_3)_2$  is the donor, and the acceptor is  $-\text{CH}=\text{C}(\text{CN})_2$  (SilaFluo, Fig. 2(a)). This dye shows a fluorescence quantum yield of 65% and has already been successfully used in high performance LSCs.<sup>17,22</sup> Fig. 2(b) shows the absorbance and fluorescence spectra of the 1.5 wt% SilaFluo embedded in the PMMA film and compares them with the transmittance spectrum normalized to a bare PMMA film. Notwithstanding the absorbance of SilaFluo that overlaps the solar emission spectrum only partially, limiting  $\eta_{\text{ABS}}$ , it shows a relatively large Stokes shift. Indeed, while the absorption peak is positioned at 478 nm, the fluorescence is centered at 620 nm, limiting re-absorption losses which commonly affect  $\eta_{\text{PL}}$ . Moreover, SilaFluo is stable under LSC working conditions and provides an excellent matching with the spectral response of the side Si-solar cells.

Two series of DBRs were fabricated with the CA-PVK and CA-HyTi/PVA pairs tuning their PBGs in different spectral regions of the fluorophore emission. Then, the DBRs were placed on the back side of the LSC with the aim to reflect photons leaving the slab from the escape cone (see Fig. 1(a)). To obtain the best performances from the DBRs, their PBGs should be spectrally tuned to the low energy side of the

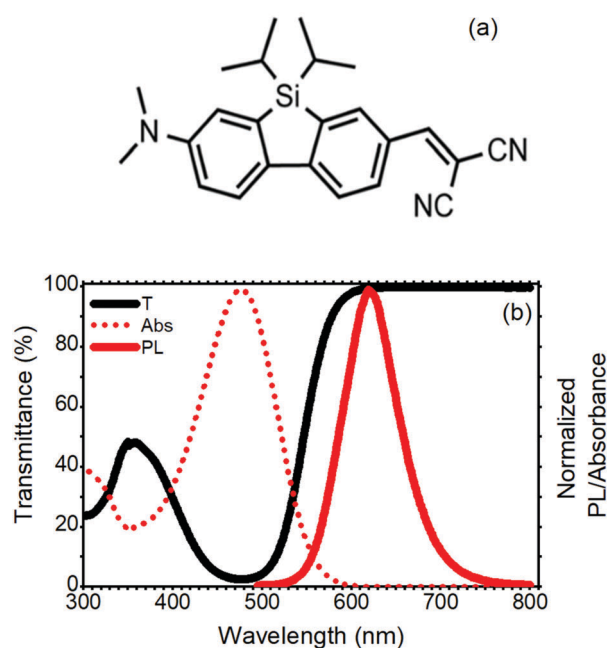


Fig. 2 (a) SilaFluo chemical structure. (b) Transmittance and normalized absorbance and photoluminescence spectra of the 1.5 wt% silaFluo-PMMA film.

1 fluorophore emission and should have a large full width at half  
 2 maximum (FWHM).<sup>27,28</sup> First, the spectral tuning and the angle  
 3 of incidence dispersion of the PBG of the DBR allow the mirrors  
 4 to work finely for all incidence geometry, *i.e.* for any daily sun  
 5 illumination conditions.<sup>9,36,42</sup> Second, a PBG FWHM larger  
 6 than the dye fluorescence spectrum is desirable to reflect all  
 7 the light escaping from the slab. Both the PBG spectral tuning  
 8 and width are mainly dictated by the periodicity and the  
 9 dielectric contrast among the DBR components.<sup>36</sup> In more  
 10 detail, the PBG position is commonly controlled by engineering  
 11 the layer thicknesses, while its spectral width is only dictated by  
 12 the dielectric contrast of the materials used. Large dielectric  
 13 contrast inorganic DBR structures usually perform best,<sup>28</sup> while  
 14 commodity polymers provide reduced dielectric contrast, but  
 15 allow very light and flexible mirrors that can be fabricated even  
 16 on the square meter area (Fig. 1(c)).<sup>36,43–45</sup> To increase the  
 17 dielectric contrast in polymer structures, several issues mainly  
 18 due to the constraint of mutual processability have to be  
 19 addressed.<sup>31,32</sup> Indeed, developing suitable high index systems  
 20 is not straightforward, while the use of low refractive index  
 21 polymers suitable for solution growth of DBRs is very  
 22 complex.<sup>35,39,46–48</sup> Only two strategies, which show relevant  
 23 drawbacks, have been reported so far. For instance, highly  
 24 porous polymers have very low refractive index,<sup>49,50</sup> but their  
 25 high void volume fraction prevents their use for the fabrication  
 26 of DBRs due to percolation of the high index counterpart within  
 27 the porosity. Low refractive index perfluorinated polymers have  
 28 been instead successfully employed to spun-cast DBRs,<sup>35,47</sup> but  
 29 the cost of such materials is very high and their processability  
 30 requires specific know-how to allow fine spectral tuning and  
 31 surface wettability. For these reasons, we decided to use CA as  
 32 the low refractive index material for DBR fabrication; in fact, it  
 33 is widely employed and easily processable.<sup>36</sup> The refractive  
 34 index of CA is about 1.47 over a broad spectral region (black  
 35 line in Fig. 3(a)). In this range, the polymer thin film does not  
 36 show absorption bands assigned to electronic transitions, which  
 37 makes it highly suitable as a transparent material for DBR  
 38 fabrication. In P series DBR, we coupled CA to PVK, which  
 39 shows relevant absorption of below 300 nm and a refractive  
 40 index value of about 1.67 (green line in Fig. 3(a)). Indeed, CA  
 41 and PVK have often been coupled in the literature for the  
 42 fabrication of polymer DBR for different applications.<sup>36</sup> Cur-  
 43 rently, PVK is the solution-processable polymer with the high-  
 44 est refractive index over a very broad spectral range available  
 45 commercially.<sup>51–54</sup> However, coupling CA and PVK does not  
 46 allow us to achieve dielectric contrast higher than 0.21, thus  
 47 limiting the PBG width. Moreover, a very large number of  
 48 periods are necessary to achieve reflectance values close to  
 49 unity.<sup>32,36,46</sup>  
 50 One of the most promising strategies to achieve a high  
 51 refractive index in polymer matrices consists in the loading of  
 52 high refractive index nanofillers such as titania nanoparticles  
 53 ( $n = 2.5$ ).<sup>55</sup> To significantly increase the complex refractive  
 54 index ( $\tilde{n}$ ) in nanocomposites suitable for photonics, two  
 55 requirements are mandatory. First, large nanofiller volume  
 fractions are needed. Second, a very small size of nanoparticles

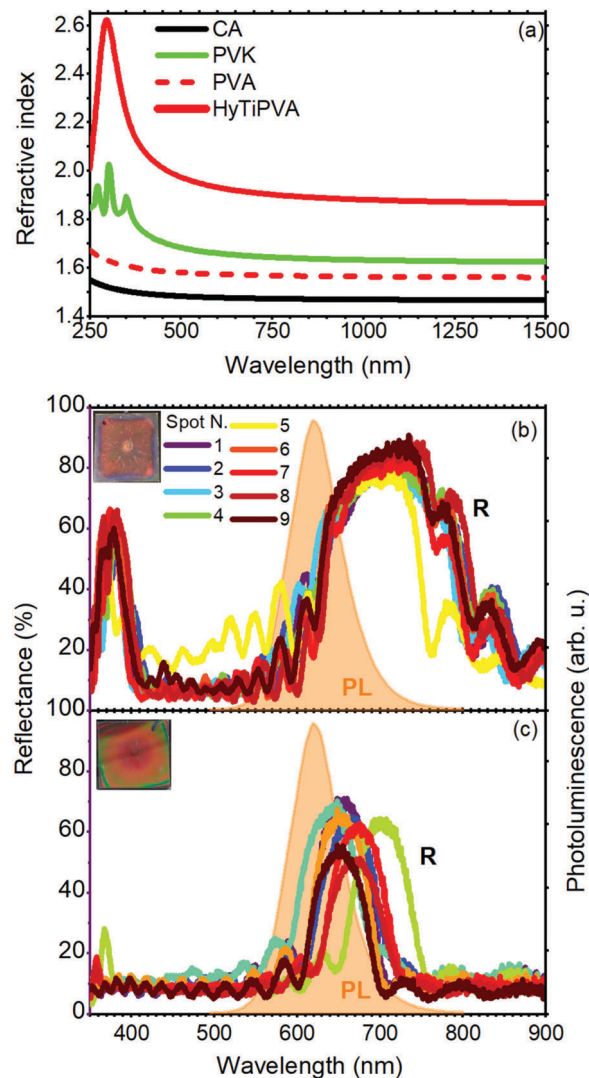


Fig. 3 (a) Refractive index of CA (black line) and PVK (green line) from the literature,<sup>41,51,52</sup> PVA (red dashed line) and HyTiPVA (red continuous line) as determined from ellipsometry measurements. (b and c) Reflectance spectra over nine different positions of the polymer DBRs made by CA-HyTiPVA and CA-PVK, respectively. In the same panels, the photoluminescence spectrum of SilaFluo is shown as dashed orange area, while the insets show the digital photographs of the samples.

and no tendency to aggregation are necessary to prevent light scattering and maintain device transparency. The combination of these requirements, along with the need for high solution processability, makes this approach challenging.<sup>56</sup> We developed a new processable material with the refractive index higher than that of PVK. To this end, we refined a method previously reported to significantly increase the refractive index of PVA, grafting hydrated titania directly to the hydroxylic group of the polymer.<sup>39,57</sup> PVA is indeed particularly appealing owing to the large amounts of hydroxylic substituents, which can be used as grafting sites for the nanofiller, thus acting as spacers, drastically reducing the aggregation processes and eliminating the need for surfactants (see Experimental section).<sup>58,59</sup> We then used the new HyTiPVA and CA to spin-cast a series (H) of



1 high performance DBRs with PBG easily tunable on the emis- 1  
sion spectrum of the LSC fluorophore. The optical response of 2  
the new HyTiPVA material was determined by spectroscopic 3  
ellipsometry, and the real part ( $n$ ) of the complex refractive 4  
index ( $\tilde{n} = n + ik$ ) is shown in Fig. 3(a) and compared with other 5  
polymers used in this work. The loading resulted in a dramatic 6  
increase of the PVA refractive index. Indeed, while bare PVA 7  
showed a refractive index of about 1.55 in the analyzed spectral 8  
range (red dashed line in Fig. 3(a)), after the loading of HyTi, 9  
the index approached 1.9 over the entire near infrared and 10  
visible spectral regions (red line in Fig. 3(a)). The full spectral 11  
response of  $\tilde{n}$  is shown in Fig. S2 (ESI<sup>†</sup>). From the spectrum 12  
reported in Fig. 3(a), according to a simple Maxwell–Garnett 13  
effective medium model<sup>55</sup> and considering the refractive index 14  
of the HyTiPVA equal to the one of anatase TiO<sub>2</sub>, we estimated a 15  
volume fraction load of at least 30%. Moreover, no absorption 16  
due to electronic transition was detected in the sample spectral 17  
range (see also Fig. S2, ESI<sup>†</sup>). These characteristics, together 18  
with the good processability of PVA, make the new composite a 19  
promising high refractive index medium to be coupled with CA. 20

The high refractive index of the HyTiPVA hybrid has a 21  
remarkable effect on the PBG FWHM. Fig. 3(b) and (c) com- 22  
pares the reflectance spectra of two DBRs made of CA and the 23  
high refractive index polymers (HyTiPVA, sample H1 in panel b; 24  
PVK, sample P1 in panel c). The reflectance spectra of the 25  
sample H1 measured in nine different spots of the sample 26  
surface show a large reflectance peak centered at 750 nm with a 27  
FWHM of 170 nm, followed by a second order peak centered at 28  
377 nm (Fig. 3(b), more spectral information and photographs 29  
are shown in Fig. S3, ESI<sup>†</sup>). Due to the deposition process, the 30  
central spot of the sample surface (spot N. 5) commonly differs 31  
from the others, affecting the surface homogeneity.<sup>29,60</sup> On the 32  
other hand, the good overlap of the other spectra, together with 33  
the interference pattern, testifies the homogeneity and the 34  
good optical quality of the sample. The presence of the second 35  
order PBG indicates that the mirrors do not fulfill the lambda 36  
fourth condition often used for laser cavities,<sup>36</sup> thus possibly 37  
allowing a wider FWHM. The background provides an average 38  
reflectance of about 10%. Comparing the reflectance spectra of 39  
the H1 DBR to the LSC emission and transmittance (Fig. 2(b), 40  
the emission spectrum is also highlighted in orange in Fig. 3(b) 41  
and (c)), we notice the tuning of the first order PBG in the 42  
emission spectral region and to its low energy side. DBRs with 43  
PBG tuned in different regions have also been fabricated and 44  
tested as reported in Fig. S4 (ESI<sup>†</sup>) for samples H2–H8. 45

The CA–PVK DBR is instead characterized by a first order 46  
PBG at 660 nm with a FWHM of 70 nm, positioned on the low 47  
energy side of the fluorophore emission (Fig. 3(c)). The second 48  
order PBG in this case has a very low intensity and is slightly 49  
visible only in two of the nine spots measured, demonstrating 50  
that the sample fulfills the lambda fourth condition.<sup>36</sup> More 51  
spectral information and images of this sample are reported in 52  
Fig. S5 (ESI<sup>†</sup>). Comparing the spectra of Fig. 3(b and c), we 53  
notice that the CA–PVK sample is less homogeneous than the 54  
one fabricated using the HyTiPVA nanocomposite. Moreover, 55  
the PBG intensity and width are smaller than for the CA–

HyTiPVA DBR but, as shown in the following, this sample 1  
provides the best performances when applied to the LSC. Fig. 2  
S6 (ESI<sup>†</sup>) shows the optical characterization of the other sam- 3  
ples of the series (P2–P8). 4

Regarding the performance of the SilaFluo–LSCs, we first 5  
focus on devices of size 24 × 24 × 3 mm<sup>3</sup>. These LSCs have a 6  
geometrical factor, *i.e.* the ratio between the illuminated sur- 7  
face area and the solar cell area, of  $G = 8$ . As described before, a 8  
diffuser layer is mounted on the back of the reference LSC with 9  
an air gap to prevent propagation losses (constant  $\eta_{\text{WG}}$ ). To 10  
assess the DBR effect on the LSC performances, we used optical 11  
efficiency ( $\eta_{\text{opt}}^{\text{LSC}}$ ) of the side cells integrated spectrally:<sup>61,62</sup> 12

$$\eta_{\text{opt}}^{\text{LSC}} = \frac{C}{G} \quad (3) \quad 15$$

where  $C$  is the concentration factor, *i.e.* the ratio between the 16  
maximum current of the PV cell attached to the LSC edges 17  
under standard solar simulator illumination and the maximum 18  
current of the bare cell placed perpendicularly to the lamp (see 19  
Experimental section and Fig. S7, S8 for details, ESI<sup>†</sup>).<sup>61,62</sup> 20

For the reference LSC, we found an optical efficiency of 9.4% 21  
(Fig. 4) with  $C = 0.75$ , in full agreement with our recent 22  
findings.<sup>17</sup> We then replaced the diffusing layer with CA– 23  
HyTiPVA (samples H). The new systems show optical efficien- 24  
cies ranging from 9.4% to 10.3% with mean 9.7% and standard 25  
deviation  $\sigma = 0.4\%$ , *i.e.* up to a 10% enhancement factor. When 26  
the diffuser is replaced with the P series of DBRs (CA–PVK), the 27  
optical efficiency of the devices is more heterogeneous and 28  
ranges from 9.3%, which is lower than the reference efficiency, 29  
to 10.6%, which represents the best enhancement achieved, the 30  
mean value achieved being 9.7% with  $\sigma = 0.5\%$ . 31

The better homogeneity of the data obtained for the H series 32  
can be explained by considering the PBG reflectance intensity 33  
and FWHM of the two systems. For the H series, the higher 34  
dielectric contrast with respect to the samples prepared with 35  
PVK allows wider PBGs and in turn their overlapping to the 36  
largest part of the fluorophore emission spectrum, even for 37  
different PBG tuning, making the H series very efficient reflec- 38  
tors for photons leaving the slab within the escape cone (Fig. 1). 39  
Then, notwithstanding possible tuning errors and a low PBG 40  
reflectance value of some of the samples at the PBG (see for 41  
instance sample H7 in Fig. S4, ESI<sup>†</sup>), all the samples prepared 42  
with the HyTiPVA composite perform better than the reference 43  
one with the diffuser. In particular, those samples tuned on the 44  
low energy side of fluorophore fluorescence and with a high 45  
FWHM (H1, H6, H8) provide the best enhancements of optical 46  
efficiency due to photon recycling of light for angle of incidence 47  
far from the normal direction. Conversely, for CA–PVK DBRs 48  
of the series P, both the PBG reflectance intensity and FWHM 49  
are relatively low. This characteristic makes the efficiency of the 50  
photon recycling more sensitive to the spectral tuning of the 51  
photonic structure. These results demonstrate that either a 52  
high dielectric contrast or a fine tuning of the photonic 53  
structure is necessary to achieve a significant enhancement of 54  
the optical efficiency of LSCs using spun-cast polymer DBRs. 55  
We would like to stress that polymer DBRs show a substantial

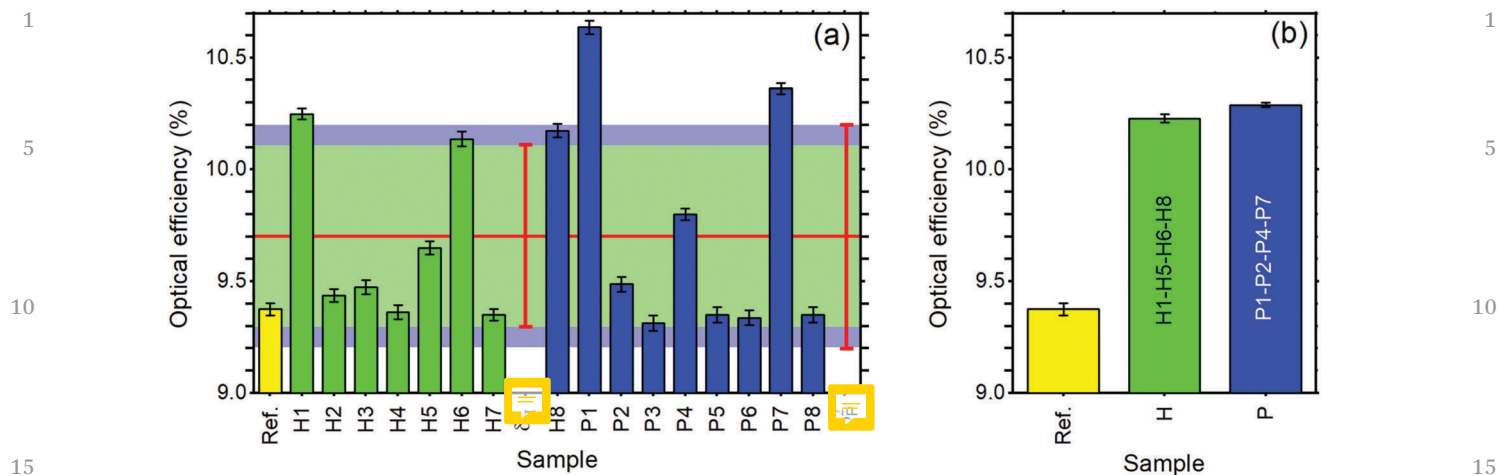


Fig. 4 (a) Optical efficiency of LSCs: reference LSC (yellow bars); LSC with applied DBR of the H (green bars) and P series (blue bars). (b) Optical efficiency of LSCs with mosaic DBR mirror. The vertical bars show  $\sigma$  for the two series of DBRs.

advantage over standard mirrors used for LSC. Indeed, these structures are much lighter, are easily adaptable to any surface (even curved if requested, Fig. 1(c)), and can be eventually grown by different techniques, such as coextrusion, over square meters at industrial level.<sup>36,43,44,63</sup>

To evaluate the scale-up opportunities of our approach, we also tested the DBRs in mosaic configuration on larger LSC, *e.g.* by doubling the LSC size ( $G = 16$ ). In this case, we created a DBR mosaic coupling the larger LSC to 4 DBR mirrors. Fig. 4(b) shows that for the larger device when the diffuser is used, the device optical efficiency does not differ from the previous case. We then exchanged the diffuser with the four best performing DBRs for each of the two series, thus enhancing the efficiency to 10.2% and 10.3% for the H and P series, respectively. Such an enhancement, which corresponds to a  $\sim 9.5\%$  increase, is impressive considering the detrimental effects of the photonic structure edges, which are known to reduce the performance of LSCs.<sup>9</sup> Again, the use of industrial techniques previously highlighted for large area DBR production could be of great help to scale up the dimension of LSCs, thus making them a widespread and successful technology.

## Conclusions

We demonstrated that polymer DBRs made of commercial polymers including CA as the low index medium and PVK or HyTiPVA nanocomposite fabricated *ad hoc* by simple wet chemistry can enhance the optical efficiency of LSCs by up to a  $\sim 10\%$  when used as back reflectors with respect to the same system with a standard diffuser. Moreover, we proved that the enhancement is retained during the scale-up of the device area by a factor of 4 and using the DBR back reflectors in mosaic configuration. The transparency in the largest part of the visible spectral range of the LSC-DBR devices, together with the possibility to fabricate these systems on the square meter area using industrial techniques, paves the way to their application

in integrated photovoltaic systems for zero energy consumption buildings in the near future.

## Author contributions

The project was conceived by D. C. and A. P. G. I. and R. F. fabricated the LSC devices and characterized their performances, P. L., S. S., A. S., and G. P. fabricated and characterized the DBR structures, M. P. performed the ellipsometric measurements, and M. S. synthesized the SilaFluo dye. Work in Genova was supervised by D. C. and M. A. A. P supervised the work in Pisa. The manuscript was written through contributions from all authors. All authors have given approval to the final version of the manuscript.

## Conflicts of interest




There are no conflicts to declare.

## Acknowledgements

Work in Genova is supported by the European Union's Horizon 2020 research and innovation program under the Marie Skłodowska-Curie Grant Agreement No. 643238. The authors also acknowledge support from the Universities of Genova and Pisa. The research leading to these results has received funding from the Università di Pisa under PRA 2017 (project No. 2017\_28) and BIHO 2017.

## Notes and references

- 1 V. Balzani and N. Armaroli, *Energy for a sustainable world*, Wiley-VCH, Weinheim, 2010.
- 2 M. G. Debije and P. P. C. Verbunt, *Adv. Energy Mater.*, 2012, **2**, 12–35.
- 3 *Nanomaterials for Sustainable Energy*, Springer, Heidelberg, 1st edn, 2016.

- 1 4 L. Wang, H. K. Bisoyi, Z. Zheng, K. G. Gutierrez-Cuevas, G. Singh, S. Kumar, T. J. Bunning and Q. Li, *Mater. Today*, 2017, **20**, 230–237.
- 5 G. Galloro, [https://www.eniday.com/it/technology\\_it/eni-ray-plus-finestre-intelligenti/](https://www.eniday.com/it/technology_it/eni-ray-plus-finestre-intelligenti/), [https://www.eniday.com/it/technology\\_it/eni-ray-plus-finestre-intelligenti/](https://www.eniday.com/it/technology_it/eni-ray-plus-finestre-intelligenti/), accessed 14/10/2018.
- 6 F. Meinardi, H. McDaniel, F. Carulli, A. Colombo, K. A. Velizhanin, N. S. Makarov, R. Simonutti, V. I. Klimov and S. Brovelli, *Nat. Nanotechnol.*, 2015, **10**, 878.
- 7 P. Moraitis, R. E. I. Schropp and W. G. J. H. M. van Sark, *Opt. Mater.*, 2018, **84**, 636–645.
- 8 F. Meinardi, F. Bruni and S. Brovelli, *Nat. Rev. Mater.*, 2017, **2**, 17072.
- 15 9 A. Bozzola, V. Robbiano, K. Sparnacci, G. Aprile, L. Boarino, A. Proto, R. Fusco, M. Laus, L. C. Andreani and D. Comoretto, *Adv. Opt. Mater.*, 2016, **4**, 147–155.
-  10 27 January 2015.
- 11 F. Meinardi, A. Colombo, K. A. Velizhanin, R. Simonutti, M. Lorenzon, L. Beverina, R. Viswanatha, V. I. Klimov and S. Brovelli, *Nat. Photonics*, 2014, **8**, 392–399.
- 20 12 I. Coropceanu and M. G. Bawendi, *Nano Lett.*, 2014, **14**, 4097–4101.
- 13 J. Mei, N. L. C. Leung, R. T. K. Kwok, J. W. Y. Lam and B. Z. Tang, *Chem. Rev.*, 2015, **115**, 11718–11940.
- 25 14 A. Pucci, *Isr. J. Chem.*, 2018, **58**, 837–844.
- 15 R. Mori, G. Iasilli, M. Lessi, A. B. Munoz-Garcia, M. Pavone, F. Bellina and A. Pucci, *Polym. Chem.*, 2018, **9**, 1168–1177.
- 16 D. Nisi, R. Francischello, A. Battisti, A. Panniello, E. Fanizza, M. Striccoli, X. Gu, N. L. C. Leung, B. Z. Tang and A. Pucci, *Mater. Chem. Front.*, 2017, **1**, 1406–1412.
- 30 17 F. Gianfaldoni, F. D. Nisi, G. Iasilli, A. Panniello, E. Fanizza, M. Striccoli, D. Ryuse, M. Shimizu, T. Biver and A. Pucci, *RSC Adv.*, 2017, **7**, 37302–37309.
- 35 18 J. Yin, D. B. Migas, M. Panahandeh-Fard, S. Chen, Z. Wang, P. Lova and C. Soci, *J. Phys. Chem. Lett.*, 2013, **4**, 3303–3309.
- 19 F. Mateen, H. Oh, W. Jung, M. Binns and S.-K. Hong, *Sol. Energy*, 2017, **155**, 934–941.
- 20 M. G. Debije, J.-P. Teunissen, M. J. Kastelijn, P. P. C. Verbunt and C. W. M. Bastiaansen, *Sol. Energy Mater. Sol. Cells*, 2009, **93**, 1345–1350.
- 40 21 J. C. Goldschmidt, M. Peters, A. Bösch, H. Helmers, F. Dimroth, S. W. Glunz and G. Willeke, *Sol. Energy Mater. Sol. Cells*, 2009, **93**, 176–182.
- 45 22 M. Carlotti, G. Ruggeri, F. Bellina and A. Pucci, *J. Lumin.*, 2016, **171**, 215–220.
- 23 P. Minei, E. Fanizza, A. M. Rodriguez, A. B. Munoz-Garcia, P. Cimino, M. Pavone and A. Pucci, *RSC Adv.*, 2016, **6**, 17474–17482.
- 50 24 J. C. Goldschmidt and S. Fischer, *Adv. Opt. Mater.*, 2015, **3**, 510–535.
-  25 J. Gutmann, J. Posdziech, M. Peters, L. Steidl, R. Zentel, H. Zappe and J. C. Goldschmidt, 2012.
- 26 A.-L. Joudrier, F. Proise, R. Grapin, J.-L. Pelouard and J.-F. Guillemoles, *Energy Procedia*, 2014, **60**, 173–180.
- 55 27 C. Ryan, P. Christian and E. F. Vivian, *J. Opt.*, 2018, **20**, 024009.
- 28 L. Xu, Y. Yao, N. D. Bronstein, L. Li, A. P. Alivisatos and R. G. Nuzzo, *ACS Photonics*, 2016, **3**, 278–285.
- 29 P. Lova, G. Manfredi, L. Boarino, A. Comite, M. Laus, M. Patrini, F. Marabelli, C. Soci and D. Comoretto, *ACS Photonics*, 2015, **2**, 537–543.
- 5 30 P. Lova, C. Bastianini, P. Giusto, M. Patrini, P. Rizzo, G. Guerra, M. Iodice, C. Soci and D. Comoretto, *ACS Appl. Mater. Interfaces*, 2016, **8**, 31941–31950.
- 31 P. Lova, V. Grande, G. Manfredi, M. Patrini, S. Herbst, F. Würthner and D. Comoretto, *Adv. Opt. Mater.*, 2017, **5**, 1700523.
- 32 G. Manfredi, P. Lova, F. Di Stasio, R. Krahne and D. Comoretto, *ACS Photonics*, 2017, **4**, 1761–1769.
- 33 P. Lova, D. Cortecchia, H. N. S. Krishnamoorthy, P. Giusto, C. Bastianini, A. Bruno, D. Comoretto and C. Soci, *ACS Photonics*, 2018, **5**, 867–874.
- 15 34 G. Manfredi, P. Lova, F. D. Stasio, P. Rastogi, R. Krahne and D. Comoretto, *RSC Adv.*, 2018, **8**, 13026.
- 35 P. Giusto, P. Lova, G. Manfredi, S. Gazzo, P. Srinivasan, S. Radice and D. Comoretto, *ACS Omega*, 2018, **3**, 7517–7522.
- 20 36 P. Lova, G. Manfredi and D. Comoretto, *Adv. Opt. Mater.*, 2018, DOI: 10.1002/adom.201800730.
- 37 P. Lova, *Polymers*, 2018, **10**, 1161.
-  38 M. Shimizu, K. Mochida, M. Katoh and T. Hiyama, *J. Phys. Chem. C*, 2010, **114**, 10004–10014.
- 25 39 M. Russo, M. Campoy-Quiles, P. Lacharmoise, T. A. M. Ferenczi, M. Garriga, W. R. Caseri and N. Stingelin, *J. Polym. Sci., Part B: Polym. Phys.*, 2012, **50**, 65–74.
- 30 40 Arduino, <https://www.arduino.cc>, accessed 10/10/2018.
- 41 WVASE32<sup>®</sup> software; b. J. A. Woollam Co., Inc.
- 42 *Organic and Hybrid Photonic Crystals*, ed. D. Comoretto, Springer International Publishing, Cham, 2015.
- 43 T. Kazmierczak, H. Song, A. Hiltner and E. Baer, *Macromol. Rapid Commun.*, 2007, **28**, 2210–2216.
- 35 44 H. Song, K. Singer, J. Lott, Y. Wu, J. Zhou, J. Andrews, E. Baer, A. Hiltner and C. Weder, *J. Mater. Chem.*, 2009, **19**, 7520–7524.
- 45 45 Chamleonlab, <https://www.chameleonlab.nl/>, <http://chameleonlab.nl/>, accessed 14/10/2018.
- 46 S. Gazzo, G. Manfredi, R. Poetzsch, Q. Wei, M. Alloisio, B. Voit and D. Comoretto, *J. Polym. Sci., Part B: Polym. Phys.*, 2016, **54**, 73–80.
- 47 2016.
- 48 T. S. Kleine, L. R. Diaz, K. M. Konopka, L. E. Anderson, N. G. Pavlopoulos, N. P. Lyons, E. T. Kim, Y. Kim, R. S. Glass, K. Char, R. A. Norwood and J. Pyun, *ACS Macro Lett.*, 2018, **7**, 875–880.
- 50 49 W. Gaëtan, F. Rolando, S. Stefan and Z. Libero, *Macromol. Chem. Phys.*, 2010, **295**, 628–636.
- 50 J. Q. Xi, M. F. Schubert, J. K. Kim, E. F. Schubert, M. Chen, S.-Y. Lin, W. Liu and J. A. Smart, *Nat. Photonics*, 2007, **1**, 176–179.
- 55 51 L. Frezza, M. Patrini, M. Liscidini and D. Comoretto, *J. Phys. Chem. C*, 2011, **115**, 19939–19946.

- 1 52 L. Fornasari, F. Floris, M. Patrini, D. Comoretto and  
F. Marabelli, *Phys. Chem. Chem. Phys.*, 2016, **18**,  
14086–14093.
- 53 L. Moroni, P. R. Salvi, C. Gellini, G. Dellepiane,  
5 D. Comoretto and C. Cuniberti, *J. Phys. Chem. A*, 2001,  
**105**, 7759–7764.
- 54 D. Comoretto, C. Cuniberti, G. F. Musso, G. Dellepiane,  
F. Speroni, C. Botta and S. Luzzati, *Phys. Rev. B: Condens.  
Matter Mater. Phys.*, 1994, **49**, 8059–8066.
- 10 55 R. J. Gher and R. W. Boyd, *Chem. Mater.*, 1996, **8**, 1807–1819.
- 56 J.-g. Liu and M. Ueda, *J. Mater. Chem.*, 2009, **19**, 8907–8919.
- 57 M. Russo, S. E. J. Rigby, W. Caseri and N. Stingelin, *J. Mater.  
Chem.*, 2010, **20**, 1348–1356.
- 58 T. Yovcheva, I. Vlaeva, I. Bodurov, V. Dragostinova and  
S. Sainov, *Appl. Opt.*, 2012, **51**, 7771–7775.
- 59 S. Mahendia, A. Kumar Tomar, P. K. Goyal and S. Kumar,  
*J. Appl. Phys.*, 2013, **113**, 073103.
- 60 G. Manfredi, C. Mayrhofer, G. Kothleitner, R. Schennach  
and D. Comoretto, *Cellulose*, 2016, **23**, 2853–2862.
- 61 Z. Krumer, W. G. J. H. M. van Sark, R. E. I. Schropp and C. de  
Mello Donegá, *Sol. Energy Mater. Sol. Cells*, 2017, **167**,  
133–139.
- 62 Y. Zhao and R. R. Lunt, *Adv. Energy Mater.*, 2013, **3**,  
1143–1148.
- 63 TORAY, <https://www.toray.com/>, <http://www.toray.com>,  
accessed 14/10/2018.

15

15

20

20

25

25

30

30

35

35

40

40

45

45

50

50

55

55